

Au-n-Type GaAs Schottky Barrier and Its Varactor Application

By D. KAHNG

(Manuscript received July 19, 1963)

Evidence is presented to show that Au-n-type GaAs rectifying contacts are majority carrier rectifiers of the Schottky type. These diodes may be characterized by a Richardson constant of 20–60 amp/cm²deg² and barrier heights of 1.03, 0.97 and 0.91 volts, corresponding to the $\langle 111 \rangle$, $\langle \overline{111} \rangle$ and $\langle 110 \rangle$ orientations of GaAs substrate.

GaAs Schottky barrier varactor diodes constructed on epitaxial films may be designed to yield a high cutoff frequency. Performance calculations in a practical case yield a "dynamic quality factor" of 50 at 6 gc under favorable conditions. A "dynamic quality factor" of about 20 at 6 gc should be obtainable with present fabrication technology.

I. INTRODUCTION

It has been demonstrated that under suitable conditions a metal-to-semiconductor rectifying contact may exhibit characteristics predictable from the simple theories advanced by Schottky¹ and Bethe.² An example of this type of system is the Au-n-type Si Schottky barrier which was reported earlier.³ In the present paper evidence is presented to show that Au-n-type GaAs is also such a case.

The main features of a metal-to-semiconductor contact are that it may be designed as a majority carrier rectifier, i.e., noninjecting rectifying junction, and that the junction is accurately describable in terms of an ideal step junction. The first feature implies that the frequency response of the diode is limited only by RC charging time or transit time rather than by minority carrier lifetime. High cutoff frequency can be achieved through the use of an epitaxial structure. Such diodes may find application in high-speed switching, microwave detection and mixing, harmonic generation, or parametric amplification using the diode as a varactor. The first of these applications, fast switching, has been discussed elsewhere.⁴

The second feature, the ideal step junction, makes the Schottky barrier highly promising as a varactor. The step junction configuration when combined with epitaxy yields advantageous varactor performance in that its capacitive sensitivity with voltage is much higher than that of a graded junction; yet no loss in Q and breakdown voltage results from the high capacitive sensitivity. The case of a retrograded junction⁵ is less favorable.

The choice of GaAs as the semiconductor part of the Schottky barrier varactor is based on two facts. First, its electron mobility is the highest among the common semiconductors available, thus allowing realization of minimum RC product while maintaining the capacitance of the unit small to facilitate diode broadband coupling to a microwave circuit. Secondly, doping close to degeneracy permits its operation at a low temperature without deterioration in performance due to carrier freeze-out.

In the following, the physical properties of the Au-n-type GaAs Schottky barrier are examined and a simple theory of a varactor design on the basis of the barrier properties is presented. The theory is used to calculate the expected performance of the varactor subject to practical considerations such as the thickness of the epitaxial layer, parasitic resistances arising from the wafer and the contact, and available pump power.

II. PHYSICAL PROPERTIES OF Au-n-TYPE GaAs SCHOTTKY BARRIER

Vacuum deposition of gold 1000 Å thick confined to a circular area of 2×10^{-3} cm² on suitably etched n-type GaAs surfaces results in diodes whose typical forward characteristics are as shown in Fig. 1. Notice that the characteristics follow the equation

$$I_f = I_s \exp [(q/kT)V] \quad (1)$$

very closely, indicating nearly ideal Schottky barrier behavior. Here I_f is the forward current, I_s the saturation current, q the electronic charge, k the Boltzmann constant, T the absolute temperature, and V the forward voltage.

Note also that I_s depends on the substrate orientation. I_s is smallest for a $\langle 111 \rangle$ -directed* substrate and increases for the $\langle \bar{1}\bar{1}\bar{1} \rangle$ and $\langle 110 \rangle$ directions in that order. This suggests that the barrier height is sensitive to GaAs orientation.

* The $\langle 111 \rangle$ direction is defined to be perpendicular to the surface which gives a smoother appearance after an etch.

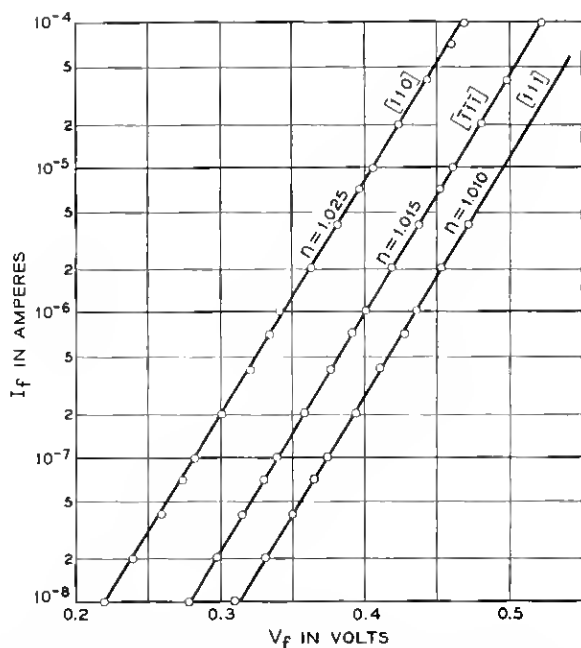


Fig. 1—Semilog plot of typical forward characteristics for three substrate orientations; n is the slope parameter, namely,

$$\frac{d(\ln I_f)}{dV_f} = \frac{1}{n} \frac{q}{kT}.$$

For a uniformly doped substrate, the barrier capacity depends on the reverse voltage in accordance with the well-known equation

$$\frac{C}{A} = \left(\frac{\epsilon q N}{2V_T} \right)^{\frac{1}{2}} \quad (2)$$

where C is the capacity, A the junction area, ϵ the permittivity, N the donor concentration, and V_T the total voltage across the junction including the built-in voltage, V_D . This is demonstrated when $1/C^2$ vs V_R (applied voltage, reverse direction positive) plots are made as shown in Fig. 2. Such plots should be linear if (2) is closely followed, and they yield information on the diffusion voltage (built-in voltage) of the barrier as well as on the ionized donor density. Table I shows data for the three orientations mentioned earlier. Two separate evaporation runs were made for each orientation. Each set of N and V_D corresponds to a single diode. For the narrow range of donor concentrations measured, the

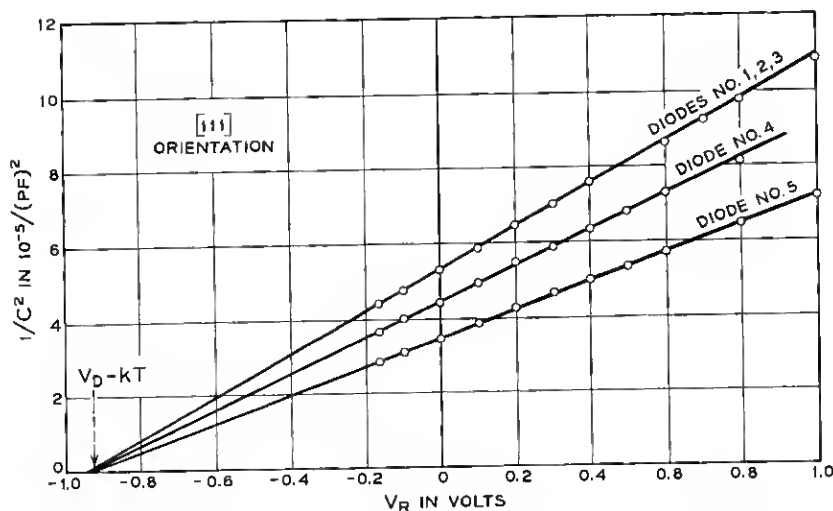


Fig. 2 — $1/C^2$ vs applied voltage for diodes constructed on (111)-oriented GaAs surface.

equilibrium Fermi level of the substrate is about $2 kT$ below the conduction band edge. The energy difference of these two levels is denoted by E_{FC} . The barrier height, ϕ , is determined from

$$\phi = V_D + E_{FC} \quad (3)$$

where $V_D = V_{\text{int}} + kT/q$ (V_{int} is the measured voltage intercept from Fig. 2. For details of this procedure see Ref. 3). Since I_s in (1) can be written as

$$I_s = A_R T^2 \exp - (q\phi/kT) \quad (4)$$

one may proceed to calculate A_R , the Richardson constant, to check the validity of the model which led to (1) and (2). I_s can be determined from the forward characteristics by plotting $[\ln I_f - (qV/kT)]$ vs I_f . The resulting calculated A_R 's are shown in the last column of Table I. The expected A_R is of the order of $100 \text{ amp/cm}^2\text{deg}^2$. Since the calculation of A_R is very sensitive to ϕ values, the results may be deemed to be in satisfactory agreement with this expectation.

It is of interest here to calculate the minority carrier contribution to the forward conduction. The hole injection efficiency, γ , can be written as⁶

$$\gamma \approx \frac{j_p}{j_s} = \frac{qp_n}{j_s} (D_p/\tau_p)^{\frac{1}{2}} \quad (5)$$

TABLE I

Orientation	N 10^{16} cm^{-3}	V_D (volts)	Φ (volts)	Ave Φ (volts)	A_R (amp/cm ² deg ²)
111	5.8	0.95	1.03	1.03	45
	5.8	0.95	1.03		
	5.8	0.95	1.03		
	7.1	0.95	1.03		
	9.02	0.94	1.02		
$\bar{1}\bar{1}\bar{1}$	7.2	0.93	1.02	0.97	20
	7.2	0.87	0.95		
	7.2	0.88	0.96		
	8.4	0.90	0.98		
	8.4	0.88	0.96		
110	5.0	0.84	0.92	0.91	20
	5.0	0.84	0.92		
	5.0	0.83	0.91		
	5.3	0.83	0.91		
	6.2	0.80	0.88		
	6.4	0.82	0.90		
	7.6	0.89	0.97		

where j_p is the hole current density, j_s the electron saturation current density, p_n the equilibrium minority carrier density of the substrate, D_p the diffusion constant of holes and τ_p the hole lifetime. The upper limit of γ estimated, using $D_p = 20 \text{ cm}^2 \text{ sec}^{-1}$, $\tau_p = 10^{-12} \text{ sec}$, and $j_s = 2 \times 10^{-11} \text{ amp/cm}^2$ for n-type GaAs of 10^{16} carrier concentration, is 5×10^{-4} . Indeed, the assumption of $\tau_p = 10^{-12} \text{ sec}$ implies that the holes do not diffuse any appreciable distance. If one makes an assumption of longer hole lifetime, γ then would be even lower than the value above. The γ calculated above applies, strictly speaking, only at the origin of the V - I curve. For high forward current range, the calculation ought to be modified to include hole drift as well as diffusion.⁷

The Au-n-type GaAs Schottky barrier then can be characterized by the set of physical parameters φ and A_R as given in Table I for the various substrate orientations. It can also be treated as a noninjecting rectifier, at least for small forward currents.

III. EPITAXIAL SURFACE BARRIER VARACTOR PERFORMANCE

Assume that the surface barrier diode is constructed on an epitaxial film of thickness d grown on a substrate material of a resistivity ρ_s . For the sake of simplicity assume that for the maximum applied reverse voltage V_m , the space charge just extends through the entire thickness d of the epitaxial n region so that

$$d = [(2\epsilon/qN)V_m]^{\frac{1}{2}} = [(2\epsilon/qN)(V_0 - V_1)]^{\frac{1}{2}}. \quad (6)$$

Here V_0 is the dc bias voltage including the built-in voltage V_D , and V_1 is the pump amplitude.

The series resistance, R_s at a voltage $V < V_m$ is given by

$$R_s = \frac{\rho_e(d-s)}{A} + R_{ss} = \frac{\rho_e}{A} (2\epsilon/qN)^{1/2} (V_m^{1/2} - V^{1/2}) + R_{ss} \quad (7)$$

where ρ_e is the resistivity of the epitaxial film, A is the junction area, R_{ss} is the contribution from the substrate and contacts, and s is the space charge width corresponding to V given by

$$s = [(2\epsilon/qN)V]^{1/2}. \quad (8)$$

The assumption used in arriving at (6) does not lead to loss of generality, since the series resistance due to unswept-out epitaxial region may be incorporated into R_{ss} in (7). The performance may now be calculated in terms of the "dynamic quality factor," \bar{Q} , of the diode as defined by Kurokawa and Uenohara.⁸ This formulation is based on the assumption that the undesired sidebands are open-circuited. Experimental results are in closer agreement with the open-circuit assumption than with the closed-circuit assumption.⁹

The figure of merit \bar{Q} as defined in Ref. 8 may be modified to include the variation of the resistance, (7), to give

$$\bar{Q} = \frac{1}{2\omega} \frac{D_1}{R_0} \quad (9)$$

where D_1 is the Fourier coefficient of the first harmonic of the elastance, $1/C$, ω is the operating frequency, and R_0 is the zero-order term of the Fourier expansion of R_s , [cf. (7)]. Equation (9) may be rewritten in combination with (2) and (7) as

$$\bar{Q} = \frac{1}{2\omega} \frac{\frac{1}{A} (2\epsilon/qN)^{1/2} \mathfrak{F}_1(V^{1/2})}{\frac{\rho_e}{A} (2\epsilon/qN)^{1/2} \mathfrak{F}_0(V_m^{1/2} - V^{1/2}) + R_{ss}} \quad (10)$$

where the symbols \mathfrak{F}_0 and \mathfrak{F}_1 are used to indicate the zero- and first-order terms of the Fourier expansion of the expression inside the brackets following the symbols. Since

$$V = V_0 + V_1 \cos \omega_p t \quad (11)$$

and

$$V_m = V_0 + V_1 \quad (12)$$

where ω_p is the angular frequency of the pump, (10) can be expressed as

$$\frac{1}{\tilde{Q}} = 2\omega\epsilon\rho_e \frac{1 - [1/(1 + \alpha)]^{\frac{1}{2}} \mathfrak{F}_0(\sqrt{1 + \alpha \cos \omega_p t})}{[1/(1 + \alpha)]^{\frac{1}{2}} \mathfrak{F}_1(\sqrt{1 + \alpha \cos \omega_p t})} + \frac{2\omega A R_{ss} (\epsilon q N / 2 V_m)^{\frac{1}{2}}}{[1/(1 + \alpha)]^{\frac{1}{2}} \mathfrak{F}_1(\sqrt{1 + \alpha \cos \omega_p t})} \quad (13)$$

where

$$\alpha = V_1/V_0. \quad (14)$$

The first term of (13) is the \tilde{Q} associated with the average loss in the epitaxial film region, and the second is the \tilde{Q} associated with the external loss. We have

$$\frac{1}{\tilde{Q}} = \frac{1}{\tilde{Q}_i} + \frac{1}{\tilde{Q}_e}. \quad (15)$$

Fig. 3 shows the pertinent values for \mathfrak{F}_0 and \mathfrak{F}_1 of $\sqrt{1 + \alpha \cos \omega_p t}$ as functions of α . Since these quantities show weak variations with α , one may take the values at $\alpha = 1$. (By definition α is never greater than unity.) Then

$$\tilde{Q}_i \cong \frac{0.58}{\omega} \frac{1}{\epsilon \rho_e} \quad (16)$$

$$\tilde{Q}_e = \frac{0.21}{\omega A R_{ss}} (2V_m / \epsilon q N)^{\frac{1}{2}} = \frac{0.21}{\omega} \frac{1}{R_{ss} C_m} = 0.21 \frac{f_m}{f} \quad (17)$$

where C_m is the minimum capacity corresponding to V_m , f_m is the cut-off frequency corresponding to C_m , and f is the operating frequency.

More accurate calculation of \tilde{Q}_i and \tilde{Q}_e is possible whenever the pumping condition is specified. Namely, when V_0 , the sum of the built-in voltage and the dc bias, and the pump amplitude are specified, the value of α is fixed. Now, corresponding to this α , more accurate numerical factors in (16) and (17) can be obtained from Fig. 3.

It is interesting to note that \tilde{Q} is a function of α but not of V_0 or V_1 separately, provided the change in R_{ss} due to changes in V_0 or V_1 is taken into account. Nonuniform epitaxial film doping would not allow the use of Fig. 3 for the numerical values in (16) and (17). However, the essential form of these equations is retained and the appropriate values of the numerical factors are calculable once the doping profile is specified.

The optimum \tilde{Q}_i is determined by smallest ρ_e one can practically use

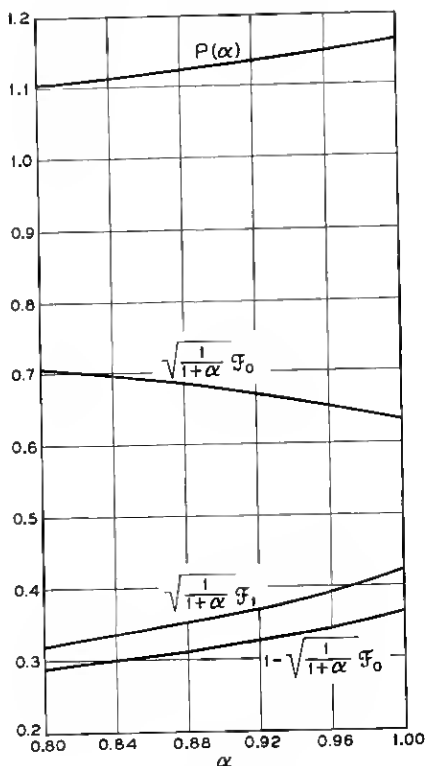


Fig. 3 — Pertinent Fourier coefficients.

$$P(\alpha) = \frac{\left(\frac{1}{1+\alpha}\right)^{\frac{1}{2}} F_1}{1 - \left(\frac{1}{1+\alpha}\right)^{\frac{1}{2}} F_0}.$$

subject to the maximum static capacity for circuit matching requirement. We now define the static capacity of the unit as

$$\bar{C} = \frac{1}{F_0(1/C)} \approx 2.8C_m \propto \frac{1}{V_m^{\frac{1}{2}}}. \quad (18)$$

Equation (18) indicates that V_m should be made as large as possible for this purpose. The extent to which V_m can be made large depends on two quantities, the breakdown voltage corresponding to a given doping level, N , and the pump amplitude. Let us examine the case where the maximum conductivity usable is limited by the breakdown voltage and the

epitaxial film thickness. The relationship between the breakdown field, E_b , assumed here to be a constant for simplicity, and the maximum space charge thickness, (or the epitaxial layer thickness), d , is

$$E_b \geq (q/\epsilon)Nd. \quad (19)$$

If d_m is the smallest thickness of epitaxial film practically attainable, then

$$1/\rho_e = \mu qN \leq (\mu \epsilon E_b/d_m) \quad (20)$$

where μ is the electron mobility. For $E_b \cdot \epsilon \approx 5 \times 10^{-7}$ volt-fd/cm² and $d_m = 10^{-4}$ cm, (20) yields an optimum doping level of 3×10^{16} cm⁻³, which corresponds to $\rho_e \approx 0.04$ ohm-cm, assuming $\mu = 5000$ cm²/volt-sec. These figures will lead to $\tilde{Q}_i \approx 390$ at 6 gc.

Now let us calculate \tilde{Q}_e , using the doping level obtained above for $A = 2 \times 10^{-5}$ cm² (0.002-inch diameter circle). Also assume that $R_{ss} \approx 0.5$ ohm. Then (17) yields $\tilde{Q}_e \approx 57$, and (15) gives a \tilde{Q} of 50.

The above calculation of dynamic quality factor was made assuming no limitations on the pump amplitudes and ideal breakdown voltage of about 25 volts. If one now assumes that only one-half of the epitaxial layer is penetrable, due to high leakage current, then \tilde{Q}_e becomes 24 and $\tilde{Q} = 22$. If one is able to reduce the epitaxial thickness to 5×10^{-5} cm, the improvement is not very significant, in that \tilde{Q}_e becomes 29 and $\tilde{Q} = 27$. In addition, if $R_{ss} = 0.8$ ohm this would affect \tilde{Q} drastically, yielding \tilde{Q} of only 17. These figures for \tilde{Q} would undoubtedly deteriorate in actual cases because the package capacity is not taken into account, although the additional external circuit loss (for instance, the cavity loss) may be incorporated in R_{ss} .

Clearly, the ultimate value of \tilde{Q} attainable is more heavily dependent on \tilde{Q}_e than on \tilde{Q}_i . \tilde{Q}_e is determined by R_{ss} and C_m . In a low-noise amplifier V_m may be advantageously made small, say about 10 volts or less. V_m should also be such that no appreciable reverse current flows. This means that the epitaxial layer thickness should be slightly larger than that dictated by (20), although \tilde{Q}_e is somewhat sacrificed. The relaxation on V_m leads to a higher optimum epitaxial layer doping than that previously calculated. This is compatible with the necessity of having the layer thickness in excess of that dictated by V_m . Equation (20) gives optimum doping of 8×10^{16} cm⁻³ or 0.02 ohm-cm for $V_m = 10$ volts and a corresponding layer thickness of 0.4μ . If the total layer thickness is 1μ (compatible with present technology), then there is a contribution to R_{ss} from the 0.6μ thick unswept-out layer. This could be partially compensated for by reducing the capacitance through use of a smaller junction area. The smallest junction area usable is, in turn, limited by the package capacity. Choice of an 0.001-inch diameter circular area leads

to an unswept-out layer resistance of 0.2 ohm and C_m , corresponding to V_m , of 0.13 pf. The total R_s then is approximately 0.8 ohm, which leads to \tilde{Q}_s of 52 at 6 gc. \tilde{Q}_s is increased to 780 by virtue of lowered epitaxial resistivity, yielding an over-all \tilde{Q} of 50 at 6 gc. These figures are optimistic, since the influence of package capacitance is again neglected.

IV. CONCLUSIONS

The Au-n-type GaAs Schottky barrier can be characterized by the physical parameters, barrier height ϕ , and Richardson's constant A_R . The values of these parameters were found to be $A_R = 20\text{--}60 \text{ amp/cm}^2 \text{ deg}^2$ and ϕ of 1.03, 0.97 and 0.91 volts, corresponding to $\langle 111 \rangle$, $\langle \bar{1}\bar{1}\bar{1} \rangle$ and $\langle 110 \rangle$ orientation. It was shown that the barrier is essentially noninjecting for small forward currents.

The combination of the surface barrier rectifying junction with a GaAs epitaxial structure may lead to a dynamic quality factor, \tilde{Q} , of 20 at 6 gc with the presently available technology. In fact, one may look forward to achieving \tilde{Q} of as much as 50 at 6 gc, either for low-voltage varactors ($V_m \leq 10$ volts) or high-voltage units ($V_m \approx 25$ volts). The latter may be useful for high-power applications such as harmonic generation, as opposed to low-noise operation, for which the former is more suitable.

V. ACKNOWLEDGMENT

The author wishes to thank M. Uenohara, with whom the applicability of the device structure was first discussed, and R. M. Ryder and J. C. Irvin for stimulating discussions. He is also grateful to A. Loya and E. W. Chase for their assistance in fabrication and measurements.

REFERENCES

1. Schottky, W., *Physik*, **118**, 1942, pp. 539-592.
2. Bethe, H. A., Theory of the Boundary Layer of Crystal Rectifiers, MIT Radiation Lab Report, 43-12, November 23, 1942.
3. Kahng, D., Conduction Properties of the Au-n-type Si Schottky Barrier, *Solid-State Electronics*, **6**, 1963, p. 281.
4. Kahng, D., and D'Asaro, L. A., *B.S.T.J.*, this issue, p. 225.
5. Chang, J. J., Forster, J. H., and Ryder, R. M., Semiconductor Junction Varactors with High Voltage Sensitivity, *IEEE Trans. Electron Devices*, **ED-10**, 1963, p. 281.
6. Henisch, H. K., *Rectifying Semiconductor Contacts*, Oxford University Press, 1957, p. 229.
7. Scharfetter, D. L., Anomalous High Minority Carrier Injection in Schottky Diodes, presented to 1963 IEEE Solid-State Device Research Conference at Michigan State University, June 12-14, 1963.
8. Kurokawa, K., and Uenohara, M., Minimum Noise Figure of the Variable-Capacitance Amplifier, *BSTJ*, **40**, 1961, p. 695.
9. Uenohara, M., private communication.